Current Research in Food Science 10 (2025) 101045

Contents lists available at ScienceDirect

Current Research in Food Science

journal homepage: www.sciencedirect.com/journal/current-research-in-food-science

Antibacterial and antibiofilm activities and mechanisms of *Toona sinensis* extracts against *Bacillus cereus* and its application in milk

Yuru Wei [a,1], Lei Lei [b,1], Honglin Jiang [c,1], Qingquan Du [a], Decheng Liu [a], Lu Chen [d], Xiaoshan Shi [a], Yanxiang Wang [a], Jingjing Li [a], Yuanliang Hu [a], Xian Xia [a,*], Junming Tu [a,**]

[a] Hubei Key Laboratory of Edible Wild Plants Conservation & Utilization, Hubei Engineering Research Center of Characteristic Wild Vegetable Breeding and Comprehensive Utilization Technology, Hubei Normal University, Huangshi, 435002, PR China
[b] Huangshi City Center for Disease Prevention and Control, Huangshi, 435000, PR China
[c] Hubei Provincial Center for Disease Control and Prevention, Wuhan, 430079, PR China
[d] Institute of Food and Nutrition Development, Ministry of Agriculture and Rural Affairs, Beijing, 100081, PR China

ARTICLE INFO

Keywords:
T. sinensis
B. cereus
Antibacterial
Antibiofilm

ABSTRACT

Bacillus cereus, a well-known foodborne pathogen, poses an increased risk because of its ability to form biofilms. In this study, we evaluated the antibacterial and antibiofilm activities of *Toona sinensis* extracts against *B. cereus*. All tested *T. sinensis* varieties demonstrated significant antibacterial activity against *B. cereus*, with inhibition zone diameters exceeding 11 mm ($P < 0.05$). Notably, the extracts from Sichuan Dazhu exhibited strong antibacterial effects, even against antibiotic-resistant *B. cereus* strains. 239 compounds were identified in Sichuan Dazhu extracts by LC-MS. The MIC and MBC of the extracts against strain ATCC 11778, BCL043 and BCL047 were 0.195 and 0.391 mg/mL, respectively. These findings were corroborated by growth curve experiments, live/dead cell staining, and scanning electron microscopy observations. Moreover, the extracts demonstrated remarkable antibiofilm activity against *B. cereus*, reducing biofilm biomass to less than 40 % ($P < 0.05$). Transcriptome analysis revealed its antibacterial and antibiofilm mechanisms. Additionally, the extracts exhibited potent antibacterial activity against *B. cereus* in skim milk. Collectively, these results underscore the significant antibacterial and antibiofilm potential of *T. sinensis* extracts, highlighting their potential applications in food safety. This report provides the first evidence of both antibacterial and antibiofilm activities in *T. sinensis* extract against *B. cereus*, while also elucidating the associated mechanisms.

1. Introduction

Bacillus cereus is a rod-shaped, Gram-positive, facultatively anaerobic bacterium (Tuipulotu et al., 2021). It is a well-known pathogen that causes toxin-induced foodborne illnesses (Jovanovic et al., 2021). Typical illness-inducing toxins of *B. cereus* are non-hemolytic enterotoxin, enterotoxin hemolysin BL, cytotoxin K, and cereulide (Huang et al., 2020). *B. cereus* usually causes two types of gastrointestinal diseases: diarrhea and emesis (Huang et al., 2020). It can also cause various local and systemic infections in humans and animals, including meningitis, endophthalmitis, endocarditis, sepsis, bone infections, and respiratory tract infections (Bottone, 2010; Tuipulotu et al., 2021). *B. cereus* is often detected in milk, dairy products, vegetables, and meat products (Choi and Kim, 2020), threatening public health and resulting in economic losses.

Moreover, it can produce endophytic spores and biofilms to cope with environmental stress (Pawluk et al., 2022). *B. cereus* biofilms contribute to alterations in nucleotides, sugars, amino acids, and energy metabolism and these alterations further participate in extracellular matrix formation, sporulation, and secondary metabolite production (Caro-Astorga et al., 2020). Biofilms attach cells to immersed surfaces or living tissues to facilitate colonization and provide protection to microorganisms from various environments (Yang et al., 2023). Spores are produced in a biofilm matrix, which makes *B. cereus* resistant to antibiotics and highly adhesive to the surfaces of food-industry-related items or raw materials (Yang et al., 2023; Zheng et al., 2017). Emetic toxins

* Corresponding author.
** Corresponding author.
E-mail addresses: xianxia@hbnu.edu.cn (X. Xia), junming_tu@hbnu.edu.cn (J. Tu).
[1] These authors contributed equally to this article.

https://doi.org/10.1016/j.crfs.2025.101045
Received 10 December 2024; Received in revised form 13 March 2025; Accepted 27 March 2025
Available online 1 April 2025

produced by *B. cereus* can attach to biofilm surfaces, increasing the risk to consumers (Huang et al., 2022). Additionally, biofilms exacerbate microbial resistance, making pathogenic microorganisms more threatening (Mlambo et al., 2022).

Food-sourced plant extracts contain several bioactive compounds that exhibit excellent antibacterial and antibiofilm activities. Extracts of pomegranate peel (Balaban et al., 2021), robusta coffee (Tritripmongkol et al., 2022), *Backhousia citriodora* (Lim et al., 2022), *Bauhinia bowkeri* (Adeyemo et al., 2022), *Lonicera japonica* Thunb (Xu et al., 2023), and grapes (Grau-Fuentes et al., 2023) have been reported to have antibacterial or anti-biofilm activity. *Toona sinensis* is an edible plant with medicinal value in Eastern and Southeastern Asia. It exhibits various activities such as antitumor, antioxidant, anti-diabetic, and anti-inflammatory activities (Peng et al., 2018). *T. sinensis* also exhibits antiviral and antibacterial effects. Its extract shows antiviral effects against SARS-CoV and H1N1 (Zhao et al., 2022). The extracts also possess promising antibacterial activities against *Esherichia coli*, *Salmonella enterica* serotype Typhimurium, *Shigella dysenteriae*, and *Staphylococcus aureus* (Yang et al., 2022; Zhao et al., 2022). Based on these studies, we speculate that *T. sinensis* may also inhibit *B. cereus*, and due to its status as an edible and medicinal plant, its application in food may be safer.

In this study, the antibacterial activity of an ethanol extracts of *T. sinensis* against *B. cereus* was evaluated using growth curve experiments, live/dead cell staining, and cell morphology observations. Antibiofilm activity was analyzed by crystal violet and fluorescein isothiocyanate (FITC) staining. Furthermore, transcriptome analysis was performed to reveal the antibacterial mechanisms. In addition, the antibacterial effect of the extracts on *B. cereus* in skim milk was evaluated.

2. Materials and methods

2.1. Strain and materials

Bacillus cereus ATCC 11778 was provided by the Hubei Provincial Center for Disease Control and Prevention (Wuhan, China). The strains BCL043 (CCTCC PB, 2025003), BCL047 (CCTCC PB, 2025004) and BCL054 (CCTCC PB, 2025005) were isolated and preserved by the Hubei Provincial Center for Disease Control and Prevention during routine surveillance of foodborne pathogenic microorganisms. The isolates were identified as *B. cereus* according to Wilson et al. (2019) by flight mass spectrometry, biochemical reaction experiments and 16S rRNA sequencing analysis (Supplemental Materials). Antimicrobial susceptibility tests showed that the isolates were multi-resistant, especially against β-lactam antibiotics (Table S1).

Mueller Hinton Agar (MHA), Mueller-Hinton Broth (MHB) and Dimethyl sulfoxide (DMSO) were purchased from Beijing Coolaber Technology Co. (Beijing, China). Fluorescein isothiocyanate (FITC) was purchased from Beijing Solarbio Science & Technology Co., Ltd. (Beijing, China). Ethanol, ethyl acetate, acetic acid, formic acid, acetonitrile and sodium chloride (NaCl) were purchased from Sinopharm Chemical Reagent Co., Ltd (Shanghai, China).

2.2. Plant materials

"Dazhu, Sichuan", "Ankang, Shaanxi", "Shiyan, Hubei", "Baise, Guangxi", and "Taihe, Anhui" varieties of *T. sinensis* were provided by the Hubei Provincial Key Laboratory of Conservation and Utilization of Edible Wild Plants (Huangshi, China).

In August 2023, freshly picked *T. sinensis* leaves were washed three times with deionized water and dried naturally in a ventilated place to remove water. The crushed leaves were extracted with 80 % (v/v) ethanol at room temperature for 24 h. The residue was processed twice, and the filtrate was collected. All filtrates were passed through a rotary evaporator (Yamato, Tokyo, Japan) and concentrated at 40 °C. The concentrated samples were then suspended in deionized water. The suspension was extracted with ethyl acetate three times to collect the organic phase extract. All extracts were dried using a rotary evaporator and concentrated at 30 °C. The dried ethyl acetate extracts were solubilized with dimethyl sulfoxide (100 % DMSO) to obtain *T. sinensis* extracts with a final concentration of 300 mg/mL (Đukanović et al., 2020).

2.3. Antibacterial activities

Antibacterial activity was screened using the agar diffusion method (Gao et al., 2020). Briefly, *B. cereus* was cultured on MHA media at 37 °C overnight and collected in 0.85 % saline solution and adjust the bacterial turbidity to 0.6 M (approximately 10^6 colony-forming units CFU/mL) by a turbidity meter (Vitek 2 DensiCHEK). Subsequently, 50 μL of bacterial suspension was evenly spread onto the MHA agar plate, and an Oxford cup (8 mm in diameter) was aseptically placed at the center of the plate. Then, 100 μL of *T. sinensis* extract (5 mg/mL in sterile ultrapure water) was carefully added into the Oxford cup. For the solvent control group, 100 μL of DMSO solution (1.7 % in sterile ultrapure water) was applied following the same procedure. All plates were incubated at 37 °C for 24 h. The diameter of the inhibition zone was measured using an electronic digital caliper (accuracy 0.01 mm) and recorded as the mean ± standard deviation.

2.4. Compositional analysis

The chemical composition of the *T. sinensis* extracts were determined by liquid chromatography-mass spectrometry (LC-MS; Agilent Technologies, Santa Clara CA, USA). The samples were separated on an Eclipse Plus C18 column (2.1 × 100 mm, 3.5 μm) with acetonitrile containing 0.1 % formic acid and ultrapure water as the eluent at a flow rate of 0.5 mL/min. The 5 % acetonitrile gradient elution was maintained for 4 min, then linearly increased to 100 % for 13 min and maintained for 3 min. The column temperature was maintained at 25 °C. The mass spectrum was scanned over a range of 100–1700 m/z, with 1.5 spectra/sec, at intervals of approximately 4 m/s and collision energies of 10, 20, and 30 eV. Compounds were identified by comparison with the National Institute of Standards and Technology database according to Gong et al. (2023).

2.5. Minimum inhibitory and minimum bactericidal concentration detection

The minimum inhibitory concentration (MIC) and minimum bactericidal concentration (MBC) of the *T. sinensis* extracts were determined using the agar dilution method (Gong et al., 2023). Briefly, the *T. sinensis* extracts were diluted in MHB medium to obtain final concentrations of 0, 0.049, 0.098, 0.195, 0.396, and 0.781 mg/mL 100 μL of bacterial suspension (approximately 10^6 CFU/mL) was inoculated in MHB medium at 37 °C, 160 rpm, and incubated for 24 h. The absorbance of the culture was then measured at 600 nm using a SpectraMax i3x multi-mode plate reader (Molecular Devices, Sunnyvale, CA, USA). The MIC was defined as the concentration at which no bacterial growth was observed. The bacterial solutions were then spread on MHA medium at 37 °C and incubated for 24 h, and the concentration at which the plate did not have colony growth was determined as the MBC.

2.6. Growth curve experiment

The *B. cereus* growth curve was determined according to the method described by Chang et al. (2023), with minor modifications. The *T. sinensis* extracts were added to 5 mL of MHB medium to a final concentration of 0, 0.5, 1, and 2 MIC, after which, 100 μL of bacterial suspension (approximately 10^6 CFU/mL) was added to the medium and incubated at 37 °C and 160 rpm for 24 h. Finally, 200 μL was removed at 2 h intervals and the absorbance was measured at 600 nm.

2.7. Live/dead cell staining

Live/dead cell staining was performed using a live/dead (N01 and PI) bacterial staining kit (Bestbio, Shanghai, China). *B. cereus* cells were observed using confocal laser scanning microscopy (CLSM) (Ren et al., 2019). Briefly, *B. cereus* cells in the logarithmic growth phase were collected and resuspended by centrifugation in sterile 0.85 % NaCl and washed three times at 4 °C (3000×*g*, 5 min). The *T. sinensis* extracts were added to bacterial suspension (approximately 10^8 CFU/mL) to a final concentration of 0, 0.5, 1, and 2 MIC at 37 °C, 160 rpm for 2 h. Samples were collected by centrifugation and washing at 4 °C (10,000×*g*, 3 min). Cells were resuspended in N01 and PI staining solutions and incubated for 15 min at room temperature in the dark. Finally, the bacteria were washed with 0.85 % NaCl and resuspended. Finally, a drop of the bacterial suspension was added to a slide and visualized using CLSM (Nikon Eclipse Ti, Tokyo, Japan).

2.8. Scanning electron microscope observation

Scanning electron microscopy (SEM) was used to observe the morphological changes in *B. cereus* cells after treatment with *T. sinensis* extracts (Sun et al., 2020). *B. cereus* cells in logarithmic growth phase were taken and resuspended by centrifugation in sterile 0.85 % NaCl at 4 °C and washed three times (3000×*g*, 5 min). *T. sinensis* extracts were added to MHB medium at final concentrations of 0, 0.5, 1, and 2 MIC. 50 μL bacterial suspension (about 10^8 CFU/mL) were inoculated into the medium at 37 °C, 160 rpm/min, and processed for 4 h. Bacteria were collected by centrifugation and washing at 4 °C (10,000×*g*, 3 min). Next, they were fixed with 2.5 % glutaraldehyde solution (Coolaber, Beijing, China) at 4 °C overnight. Bacteria were centrifuged in sterile 0.85 % NaCl, 4 °C, and washed three times after fixation (3000×*g*, 5 min). The samples were dehydrated using a gradient of 30 %, 50 %, 70 %, 80 %, 90 %, and 100 % (v/v) ethanol, and finally dehydrated twice with anhydrous ethanol at room temperature to completely remove water from the samples for freeze-drying. After a series of steps, the bacteria were examined using SEM (Hitachi S-4800, Tokyo, Japan).

2.9. Inhibition of biofilm

2.9.1. Determination of bacterial biofilm biomass

Biofilm biomass of *B. cereus* was determined using crystal violet staining (Kang et al., 2018). The *T. sinensis* extracts were diluted in MHB medium to final concentrations of 0, 0.5, 1, and 2 MIC (0 MIC was used as control group). Then, 10 μL of *B. cereus* suspension (approximately 10^6 CFU/mL) was inoculated in 96-well plates, after adding 90 μL of medium to each well, and incubated at 37 °C at rest for 24 h. After a biofilm was formed, it was gently washed three times with 20 mmol/L phosphate-buffered saline (PBS) and fixed with methanol for 15 min. Next, the samples were stained with crystal violet (Beyotime, Shang, China) for 30 min and washed gently with PBS three times to remove the unbound stain. Finally, crystal violet was fully solubilized with 33 % (v/v) acetic acid, and the absorbance was measured at 590 nm. The biofilm content ration = [Experiment group absorbance - Control group absorbance]/Control group absorbance × 100 %.

2.9.2. Observation of bacterial biofilms

Light microscopic observation of *B. cereus* biofilms was performed as described in Section 2.9.1. The biofilms were stained with crystal violet after formation, washed with PBS to remove the unbound staining solution, evaporated to dryness, and viewed under a light microscope (Aseet, Suzhou, China) according to Bai et al. (2019).

The antibiofilm activity of the *T. sinensis* extracts were further observed using fluorescence microscopy, following the method of Li et al. (2023), with slight modifications. In the presence of *T. sinensis* extract, the bacteria formed biofilms after static incubation. Then, the membrane was gently washed three times with PBS to remove planktonic bacteria, and stained with FITC (20 μL, 5 mg/mL) for 30 min. The membrane was gently washed to remove unbound dye and visualized under an inverted fluorescence microscope (Nikon Eclipse Ti 2, Tokyo, Japan).

2.10. RNA isolation and sequencing

T. sinensis extracts were dissolved in MHB medium to a final concentration of 0.5 MIC, and 2 mL of bacterial suspension (approximately 10^8 CFU/mL) was added and the samples were incubated at 37 °C and 160 rpm, for 8 h. *B. cereus* grown without the addition of extracts was used as a control. Bacteria were collected, and total RNA was extracted. Sequencing libraries were constructed and sequenced by Shanghai Chengqi Biological Biotechnology Co. (Shanghai, China). RNA-Seq sequencing had been submitted to the NCBI Sequence Reading Archive with accession number PRJNA 1107356. After quality control, high-quality data (clean reads) were used for subsequent analysis. Expression analysis to identify differentially expressed genes (DEGs) was performed using edgeR. To eliminate biological differences, DEGs were identified based on a threshold of $p < 0.05$, and $|\log2(\text{fold change})| > 1$. Gene Ontology (GO) functional and Kyoto Encyclopedia of Genes and Genomes (KEGG) pathway enrichment analyses were performed using topGO and ClusterProfiler, respectively (Zhou et al., 2023).

2.11. Quantitative reverse transcription PCR (RT-qPCR)

The bacterial culture conditions and *T. sinensis* extract treatment were maintained consistently with those used in the transcriptome experiment (see Section 2.10). Cells were harvested by centrifugation at 8000 rpm for 10 min at room temperature. Total RNA was extracted using the TRIzol™ Plus RNA Purification Kit (ThermoFisher Scientific, Waltham, MA, USA), and genomic DNA was subsequently removed using the gDNA Eraser (TaKaRa, RR047A, Dalian, China). Complementary DNA (cDNA) was then synthesized via reverse transcription using the PrimeScript RT Reagent Kit (TaKaRa, RR047A, Dalian, China). The resulting cDNA was quantified by RT-qPCR using the SuperStar Universal SYBR Master Mix (Jiangsu CoWin Biotech Co., Ltd., Taizhou, China), with an annealing temperature of 60 °C and a total of 40 amplification cycles. The primers used are listed in Table S2. RT-qPCR was performed on a Bio-Rad Touch Real-time PCR CFX96 system (Bio-Rad, California, USA) (Ren et al., 2019).

2.12. Sterilization experiments of T. sinensis extracts in milk

The *T. sinensis* extracts were tested for its bacteriostatic effect in skim milk, as previously described (Wang et al., 2022). The *T. sinensis* extracts were added to commercially available autoclaved skim milk (Yili, Inner Mongolia, China) at final concentrations of 1.5, 3, and 6 mg/mL. Skimmed milk without the extracts were used as a control. The milk was then inoculated with *B. cereus* (10^3–10^4 CFU/mL) and incubated at 37 °C and 160 rpm for 48 h. Samples were taken at intervals of 0, 3, 6, 9, 12, 24, and 48 h and counted by plate counting on MHA medium.

2.13. Data analysis

All experiments were performed in triplicate. Data analysis was performed using one-way ANOVA in SPSS software (version 26.0; IBM Corp. Armonk, NY, USA). Post hoc multiple comparisons were conducted using Tamhane's test for the data in Table S3 and Duncan's test for the data in Fig. 5, and statistical significance was set at $p < 0.05$. Additionally, the data in Fig. S2 were analyzed using independent samples t-tests ($p < 0.05$). The results are expressed as the mean ± standard deviation.

3. Results and discussion

3.1. Antimicrobial effects of extracts from different varieties of T. sinensis

Different varieties of *T. sinensis* extracts exhibited antibacterial activity against *B. cereus* strains (Table S3). In the disc diffusion assay, the diameters of the inhibition zones of extracts from all five *T. sinensis* species against *B. cereus* were greater than 11 mm, and the diameters of the inhibition zones of "Sichuan Dazhu" was larger than that of other species. Based on the color of the plant, *T. sinensis* can be classified into two types: red and green (Zhao et al., 2023). "Sichuan Dazhu" is a red toon. Compared with green toons, red toons show higher biological activity and nutritional value (Su et al., 2020). Therefore, the red variety, "Sichuan Dazhu", was selected to inhibit *B. cereus* for subsequent experiments.

3.2. Compositional analysis of T. sinensis extracts

Biochemical analysis of *T. sinensis* extracts using LC-MS identified 239 compounds (Table S4). A total of 73 compounds with a similarity score greater than 0.8 were selected for analysis. The compounds were divided into the following 13 categories: flavonoids (27.40 %), amino acids and their derivatives (19.18 %), alkaloids (16.44 %), lipids (13.70 %), carbohydrates (6.85 %), polyphenols (5.48 %), and terpenoids (2.74 %) (Fig. 1). Flavonoid secondary metabolites are the main substances of *T. sinensis* extracts with good antimicrobial activity (Shamsudin et al., 2022). The compounds detected in the extracts of *T. sinensis* were consistent with the results of previous studies, which identified quercetin, kaempferol, gallic acid, rutin (Wang et al., 2007), isoquercetin, myricetin (Peng et al., 2018), hyperoside (Zhao et al., 2022). The potential antibacterial and antibiofilm compounds were analyzed (see below 3.3 and 3.4).

3.3. Antibacterial activity of T. sinensis extracts against B. cereus

The MIC and MBC of the *T. sinensis* extracts against strain ATCC 11778 were 0.195 and 0.391 mg/mL, respectively. Additionally, for the drug-resistant *B. cereus* strains BCL043 and BCL047, the MIC and MBC values were identical to those of strain ATCC 11778. For *B. cereus* BCL054, the MIC was 0.195 mg/mL, while the MBC exceeded 6.25 mg/mL (Fig. 2). Based on the MIC and MBC results, *T. sinensis* extract exhibited inhibitory effects on all four *B. cereus* strains tested in the study, though its efficacy varied among the different strains. Strain ATCC 11778 was used for subsequent experiments.

To further investigate the inhibitory effect of *T. sinensis* extracts on *B. cereus*, we monitored the growth of *B. cereus* in the presence different concentrations of *T. sinensis* extracts over a 24 h period (Fig. 3). Compared to the control group, the *T. sinensis* extracts significantly inhibited the growth of *B. cereus*. Moreover, the inhibitory effect became more pronounced with increasing concentrations. During the logarithmic phase, 0.5 MIC partially inhibited bacterial growth, whereas 1 MIC and 2 MIC almost completely suppressed the growth of *B. cereus*, indicating potent antibacterial activity.

A live/dead cell staining assay was performed. The green fluorescent probe N01 could cross the living cell membrane and bind to nucleic acids, and the red fluorescent probe PI stains only dead cells with damaged membranes. As shown in Fig. 4A, the cells in the control group exhibited intense green and faint red fluorescence, indicating the predominance of live cells over dead cells. Conversely, the experimental groups (0.5, 1, and 2 MIC) demonstrated a progressive reduction in the number of live cells and a concomitant increase in the number of dead cells with increasing concentrations of the *T. sinensis* extract.

SEM was used to examine cell morphology following treatment with the *T. sinensis* extracts (Fig. 4B). In the control group, *B. cereus* displayed a typical rod-shaped morphology, with a smooth surface and an intact structure. However, exposure to 0.5, 1, and 2 MIC led to cell rupture, content leakage, and disruption of cellular integrity. Moreover, the extent of cellular fragmentation increased with increasing concentrations of *T. sinensis* extract.

These results suggest that *T. sinensis* extracts exhibit excellent antibacterial activity against *B. cereus*. Previous studies have reported the MICs of various plant extracts against *B. cereus*. Fei et al. (2019) found that the MIC of an olive oil polyphenol extracts was 0.625 mg/mL, whereas Akinpelu et al. (2015) reported that the MIC of a *Persea americana* extracts against *B. cereus* was 25 mg/mL. Tritripmongkol et al. (2022) determined the MIC of robusta coffee extracts against *B. cereus* to be 2 mg/mL. In comparison, the *T. sinensis* extracts potently inhibited *B. cereus* growth, with an MIC of 0.195 mg/mL, demonstrating superior efficacy compared to other reported extracts from these plants. In terms of natural antibacterial compounds, *T. sinensis* extract exhibited a lower MIC against *B. cereus* compared to thymol (MIC 0.625 mg/mL) (Wang et al., 2022), while its MIC and MBC values were comparable to those of carvacrol (MIC 0.19 mg/mL, MBC 0.38 mg/mL) (Li et al., 2025). This highlights the promising potential of the *T. sinensis* extracts as an effective antibacterial agent against *B. cereus*. LC-MS analysis revealed that *T. sinensis* extracts contained catechins, luteolin, quercetin, and kaempferol, which have been reported to exhibit antibacterial activity against *B. cereus* (Friedman et al., 2006; Xu et al., 2023). Additionally, studies also have shown that compounds such as astragalin inhibit the growth of *Candida albicans* (Ivanov et al., 2020). Hyperoside and gallic acid show antibacterial and antibiofilm effects against *Escherichia coli* (Abouzeid et al., 2023; Tian et al., 2022), while isoquercitrin and myricetin possess antimicrobial activity against *Staphylococcus aureus* (Gao et al., 2020; Wang et al., 2020). These results indicated that the extracts of *T. sinensis* have good antimicrobial activity.

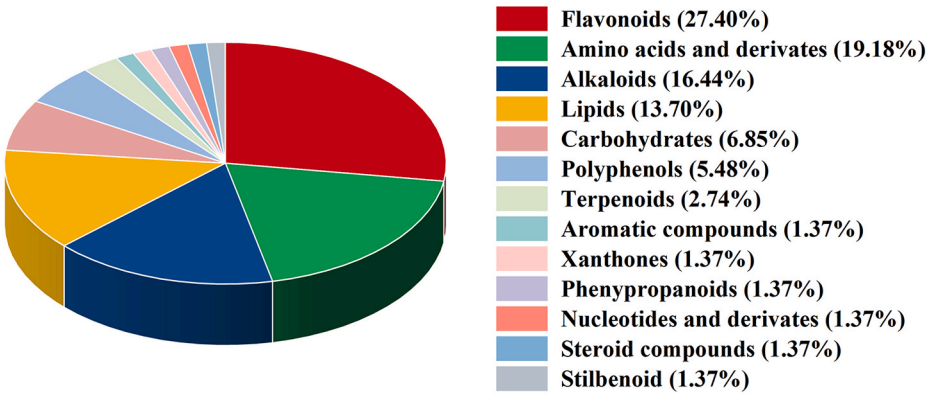

Fig. 1. Types and proportions of the phytochemicals identified from *T. sinensis* extracts.

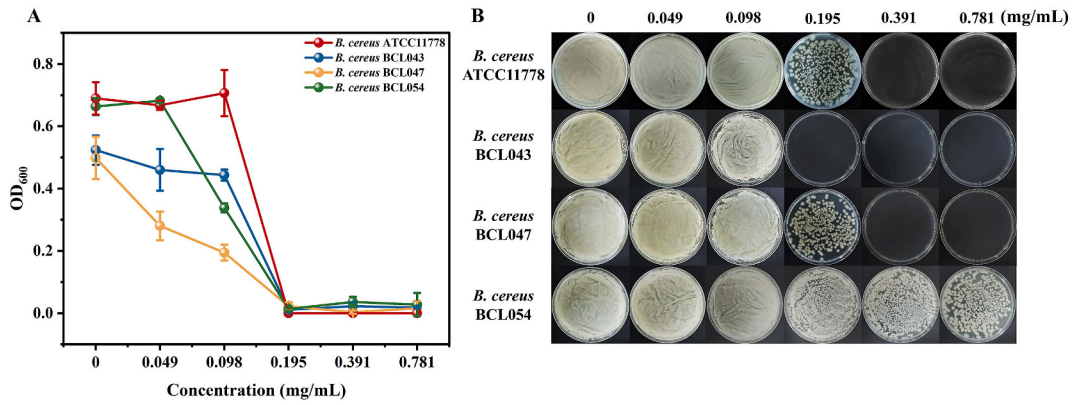

Fig. 2. The MIC (A) and MBC (B) of *T. sinensis* extracts against *B. cereus* strains ATCC11778, BCL043, BCL047, and BCL054.

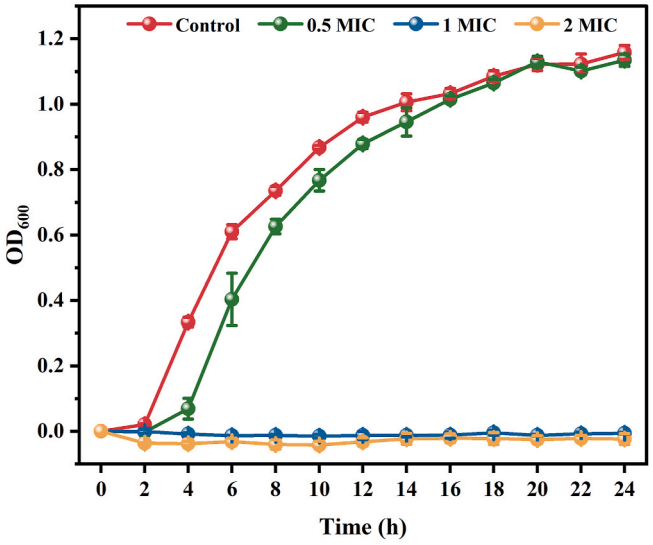

Fig. 3. The growth curves of *B. cereus* ATCC11778 with 0, 0.5, 1 and 2 MIC *T. sinensis* extracts. Data were expressed as mean ± standard deviation (n = 3).

3.4. Antibiofilm activity of T. sinensis extracts

Biofilm formation was observed in cells grown in 96-well plates after staining with crystal violet. The color significantly faded after treated with *T. sinensis* extracts at concentrations of 0.5, 1, and 2 MIC. Further quantitative analysis based on absorbance values indicated that the biomasses of the biofilms treated with *T. sinensis* extracts at concentrations of 0.5, 1, and 2 MIC extracts were 31.95 %, 27.76 %, and 23.10 %, respectively (Fig. 5A). This indicates that the *T. sinensis* extracts exhibited excellent antibiofilm activity. This result was further confirmed by observing the biofilms using light and inverted fluorescence microscopy (Fig. 5B). Previously, ursolic acid (Son and Lee, 2020) and gallotannins (Gan et al., 2018) in *T. sinensis* have been shown to inhibit biofilm formation by *S. aureus*. In addition, quercetin is known to inhibit biofilm formation in a variety of pathogenic bacteria by inhibiting biofilm-formation related pathways such as bacterial adhesion, quorum sensing, and nucleic acid synthesis (Memariani et al., 2019). These components might be the reason why *T. sinensis* extracts possessed the antibiofilm ability against *B. cereus*.

3.5. RNA sequencing data analysis

To further investigate the mechanism of inhibition of *T. sinensis* extracts against *B. cereus*, we performed transcriptome analysis. The samples were subjected to Illumina sequencing, and after filtering out low-quality reads, the Q20 value of the samples was >97 %, indicating that the sequencing was of high quality and could be analyzed in the next step. Compared to the control group, 1740 DEGs were identified in the experimental group. A volcano plot was used to demonstrate the distribution of the DEGs (Fig. 6A), with the horizontal coordinate representing the fold change in gene expression differences and the vertical coordinate representing the statistical significance of gene expression differences. A total of 787 genes were downregulated, as indicated by blue dots and 953 genes were upregulated, as indicated by red dots (Fig. 6B). The gray dots indicate genes with no significant differences.

3.5.1. GO enrichment analysis

GO enrichment histograms were used to reflect the distribution of the number of DEGs enriched in biological processes, cellular components, and molecular functions. There were 474 terms related to biological processes, 62 terms related to cellular components, and 109 terms related to molecular functions. We selected the 30 GO terms with the most significant enrichment, as shown in Fig. 7A. Among the 30 GO terms, 26 belonged to the biological process category, including 20 associated with nucleotide metabolism. This suggested that the *T. sinensis* extracts might disrupt nucleotide metabolism. The inhibition of nucleotide synthesis is a crucial pathway for antibiotic development. The ability of kaempferol, and luteolin to interfere with DNA synthesis in *Staphylococcus aureus* or *Treponema pallidum* by inhibiting DNase has been reported (Huang et al., 2015; Zhang et al., 2022). In addition, the decomposition of organic acids, the tricarboxylic acid (TCA) cycle, acetyl-CoA metabolism, amino acid degradation, and thioester metabolism in *B. cereus* were also influenced by the *T. sinensis* extract. Carbohydrate metabolism (TCA cycle and acetyl-CoA metabolism) and thioester metabolism play important roles in providing energy for cellular growth and supplying raw materials for synthetic metabolism (Wang et al., 2023). The decomposition of organic acids and amino acid degradation can also provide energy to cells while generating important intermediate products (McCalley et al., 2019; Zaunmüller et al., 2006). Additionally, both the cellular component and molecular function categories of the GO terms were associated with the ribosome, which serves as the site for protein synthesis and is also a target for antibiotic design (Lin et al., 2018). In summary, *T. sinensis* extracts might inhibit the growth of *B. cereus* by interfering with nucleic acid metabolism, decomposition of organic acids, carbon mechanisms [tricarboxylic acid cycle, acetyl-CoA metabolism], amino acid metabolism, thioester metabolism, protein synthesis, according to GO enrichment analysis.

3.5.2. KEGG enrichment analysis

To further elucidate the regulatory role of the DEGs, we classified them to explore the enrichment of significant DEGs within the KEGG database. Compared with controls, 1740 differential genes were

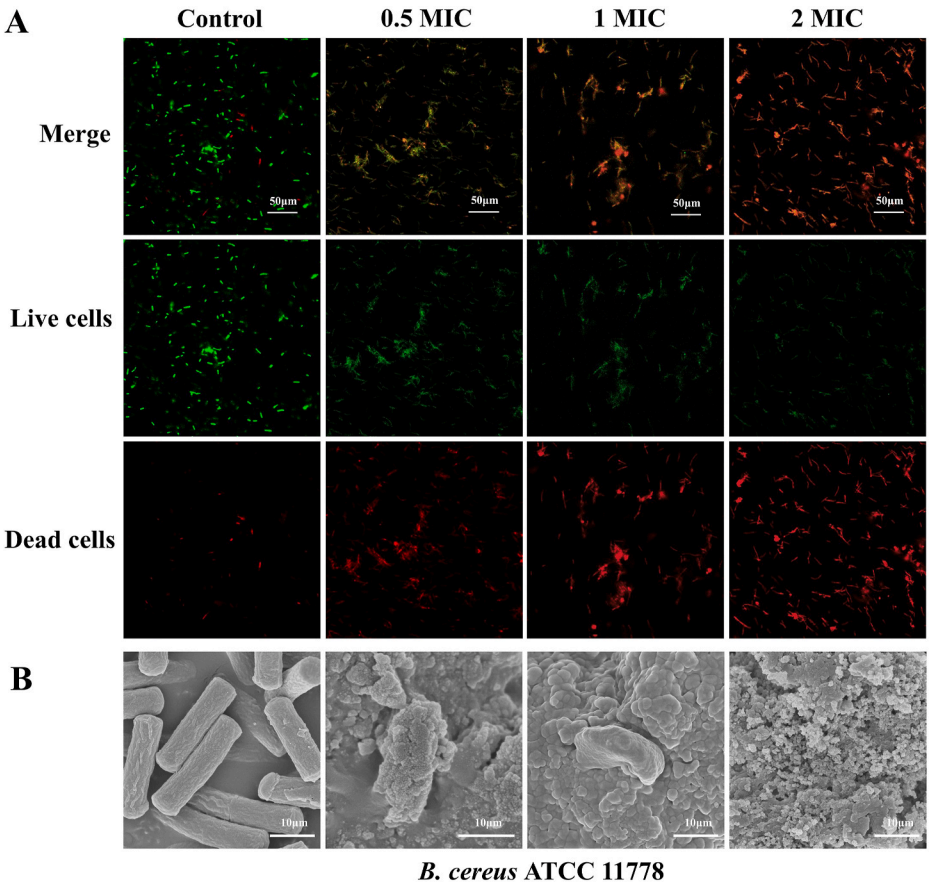

Fig. 4. Effect of *T. sinensis* extracts on the cellular integrity of *B. cereus*. (A) CLSM images of *B. cereus* treated with 0, 0.5, 1 and 2 MIC *T. sinensis* extracts. Red presented as dead cells, while green presented as live cells. (B) SEM images of *B. cereus* treated with *T. sinensis* extracts at concentrations of 0, 0.5, 1 and 2 MIC, respectively.

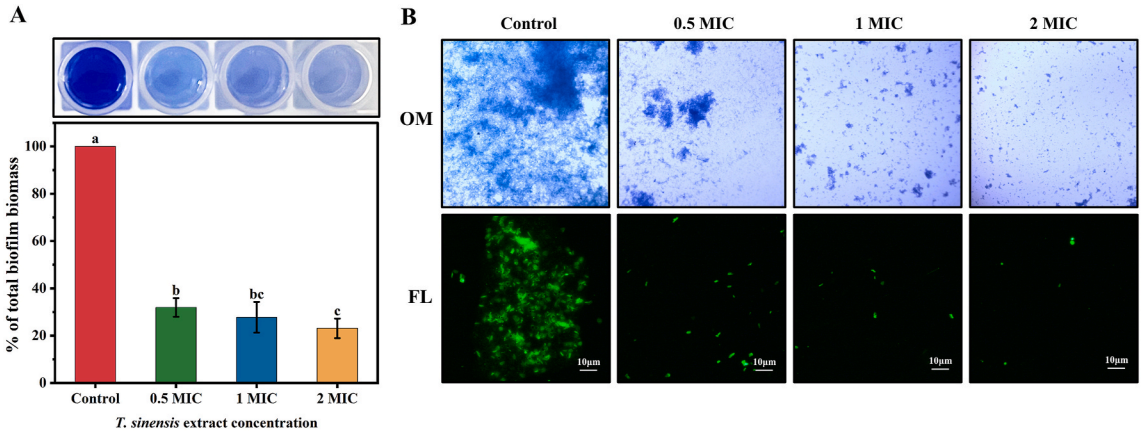

Fig. 5. Effect of *T. sinensis* on the biofilm formation of *B. cereus*. (A) The images and biofilm biomass of *B. cereus* at 0, 0.5, 1 and 2 MIC concentrations of *T. sinensis* extracts. (B) Biofilm images of *B. cereus* stained with crystal violet and fluorescein isothiocyanate, treated with 0, 0.5, 1, and 2 MIC concentrations of *T. sinensis* extracts. These were observed using an optical microscope (light microscope images at 40 times magnification) and a fluorescence microscope, respectively. Different lowercase letters indicated significant differences in biofilm biomass under different concentrations of *T. sinensis* extracts ($P < 0.05$).

enriched in 95 pathways, and the 20 pathway entries selected with the smallest *p*-values were visualized using scatter plots (Fig. 7B). The most enriched pathways in the DEGs were the biosynthesis of secondary metabolites, biosynthesis of antibiotics, and carbon metabolism, followed by ribosome, pyruvate metabolism, purine metabolism, and TCA cycle pathways. The upregulation of some secondary metabolite biosynthesis pathways and may contribute to cell decay (Liu et al., 2016). The impact on carbon (pyruvate metabolism and the TCA cycle) (Kaberdina et al., 2019; Kwong et al., 2017), nucleotide (purine metabolism) (Diehl et al., 2022), and protein metabolism (ribosome) (Ling et al., 2022) also affected the normal growth of cells. KEGG enrichment suggested that *T. sinensis* extracts might lead to the accumulation of secondary metabolites in cells, while reducing resistance to antibacterial substances. *T. sinensis* extracts might disrupt pyruvate metabolism and purine metabolism. The results of KEGG enrichment analysis further validated the findings of GO enrichment analysis. In general, the extracts

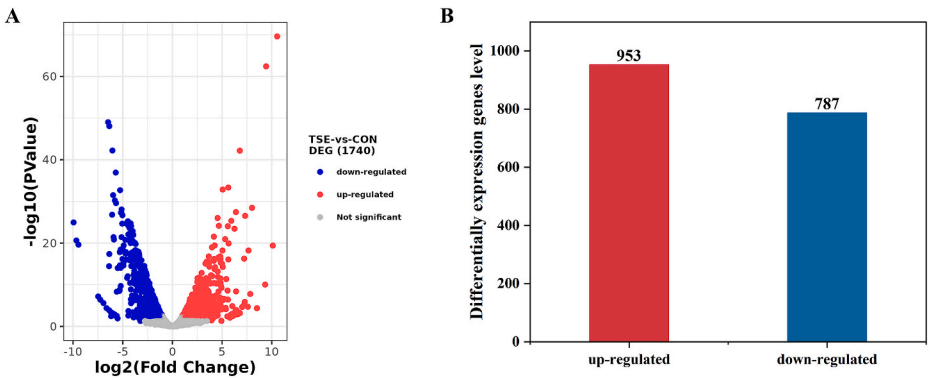

Fig. 6. The volcano plot for the differentially expressed genes (A) and number of up-regulated and down-regulated genes (B) in *B. cereus* treated with 1/2 MIC *T. sinensis* extracts for 8 h.

affected the nucleic acid metabolism, protein metabolism, carbon metabolism, thiol metabolism, and synthesis of metabolites in *B. cereus* (Fig. 8).

3.5.3. Genes associated with biofilm formation

Among the genes with altered expression levels, nine were downregulated (*carA*, *carB*, *smPurL*, *purQ*, *PNP*, *hutI*, *hutU*, *fliK*, and *fhuD*), whereas two upregulated genes (*ltaS* and *padR*) were associated with biofilm formation (Fig. 9). The synthesis of biological membranes can be divided into four steps (attachment, microcolony, development and maturation, and dispersion).

The *smPurL*, *purQ*, and *PNP* genes play indispensable roles in purine biosynthesis, a process crucial for eDNA synthesis. Inhibiting eDNA synthesis subsequently interferes with the attachment stage of biofilm formation (Gélinas et al., 2021). In particular, the *PNP* gene is the target of drugs used for the prevention of biofilm inhibition (Koopman et al., 2015). Similarly, the histidine biosynthesis pathway, which has been implicated in the attachment step of biofilm formation, is also targeted for drug development to inhibit biofilm formation (Ding et al., 2018). Here, *hutI and hutU* genes, involved in histidine biosynthesis, were found to be downregulated after treatment with *T. sinensis* extracts. Flagella was also associated with the attachment of biofilm formation. The *fliK* gene is associated with the synthesis of flagella, while *carA*, *carB*, and *padR* are associated with the movement of flagella. In *Pseudomonas plecoglossicida* and *Bacillus licheniformis*, *fliK* is crucial for biofilm formation and contributes to its pathogenicity (Liu et al., 2022; Wang et al., 2020). The *carA* and *carB* genes encode the small and large subunits of carbamoyl-phosphate synthase (CPS), respectively, which are required for biofilm formation (Zhuo et al., 2015). The *padR* gene encodes a repressor that regulates phenolic acid decarboxylase expression (Park et al., 2017), and phenolic compounds can affect flagella movement and further result in the inhibition of biofilm formation (Buchmann et al., 2023).

Additionally, the iron-uptake-related gene *fhuD* was downregulated. Iron metabolism is involved in microcolony step of biofilm formation (Zhang et al., 2021). The *ltaS* gene encodes lipoteichoic acid synthase, which produces lipoteichoic acid, which affects microcolony, development and maturation, and dispersion of biofilm formation (Ahn et al., 2018).

3.6. RT-qPCR analysis

In this study, RT-qPCR was used to further validate the transcription levels of key genes associated with antibacterial and antibiofilm activities, as identified through transcriptomic analysis. The qPCR results revealed that *nadA* and *pyrC*, which are involved in carbon metabolism (Zhu et al., 2021) and nucleic acid metabolism (Truong et al., 2013), respectively, were upregulated. In contrast, *acrD* and *MDR*, associated with biological fitness (Fulde et al., 2014) and the extrusion of multiple antimicrobial drugs (Zhang et al., 2020), were downregulated. Regarding biofilm formation, *carB*, *fliK*, *purQ*, and *hutI* were downregulated (Fig. S2), potentially reducing biofilm attachment ability (Park et al., 2017). Meanwhile, the upregulation of *padR* and *ltas* (Fig. S2) may inhibit microcolony development, maturation, and biofilm dispersion (Buchmann et al., 2023). These findings are consistent with the transcriptomic data.

3.7. Application of T. sinensis extracts in skimmed milk

These results demonstrated the significant inhibitory effect of *T. sinensis* extracts on *B. cereus*. Considering that dairy products are prone to contamination with *B. cereus*, it is important to assess the inhibitory potential of *T. sinensis* extracts in skimmed milk. As illustrated in Fig. 10, the growth of *B. cereus* in skimmed milk without extracts reached a plateau after approximately 12 h with a bacterial count of 8.18 logs. When 3 mg/mL of *T. sinensis* extract was added, the bacterial count decreased to 7.26 logs after approximately 48 h. Remarkably, when 6 mg/mL extract was added, *B. cereus* cells were completely inhibited and eradicated within 12 h.

In milk preservation experiments, the antimicrobial effect of the extract was evaluated by factors such as concentration, treatment duration, and the number of viable bacteria. Studies have shown that live *B. cereus* could still be detected after 7 days of treatment with 4 mg/mL of *Polygonatum sibiricum* extracts (Fei et al., 2023). However, 3 mg/mL of *T. sinensis* extract inhibited bacterial growth within 12 h, and a 6 mg/mL concentration achieved a bactericidal effect, reducing the number of viable bacteria to the detection limit at 12 h. Besides, the MIC of *T. sinensis* extract against *B. cereus* in this study was lower than that of olive oil polyphenol, *Persea americana* extracts, robusta coffee extracts (Akinpelu et al., 2015; Fei et al., 2019; Tritripmongkol et al., 2022). This indicated that the extracts of *T. sinensis* had some advantages over other reported crude substances in the application against *B. cereus*. Moreover, the bactericidal efficacy of *T. sinensis* extract against *B. cereus* was notably superior compared to some compounds. Rhamnolipid at a concentration of 6.25 mg/mL reduced the number of viable bacteria to below the detection limit after 70 h (Bertuso et al., 2022), while 5 mg/mL of sucrose laurate inhibited only the growth of *B. cereus* within 10 days (Ning et al., 2022). *T. sinensis* has also been widely recognized as a natural antioxidant (Wang et al., 2007), highlighting its potential as a valuable and multiple function food additive, all of which indicate the advantages of *T. sinensis* as a food additive. These results indicated the potential application of *T. sinensis* extracts as antimicrobials in dairy products.

The limitations of this study are: (1) the specific active components in the extracts are not yet clear. (2) Although *T. sinensis* is an edible plant, there is a lack of safety evaluation, as safety may be related to the

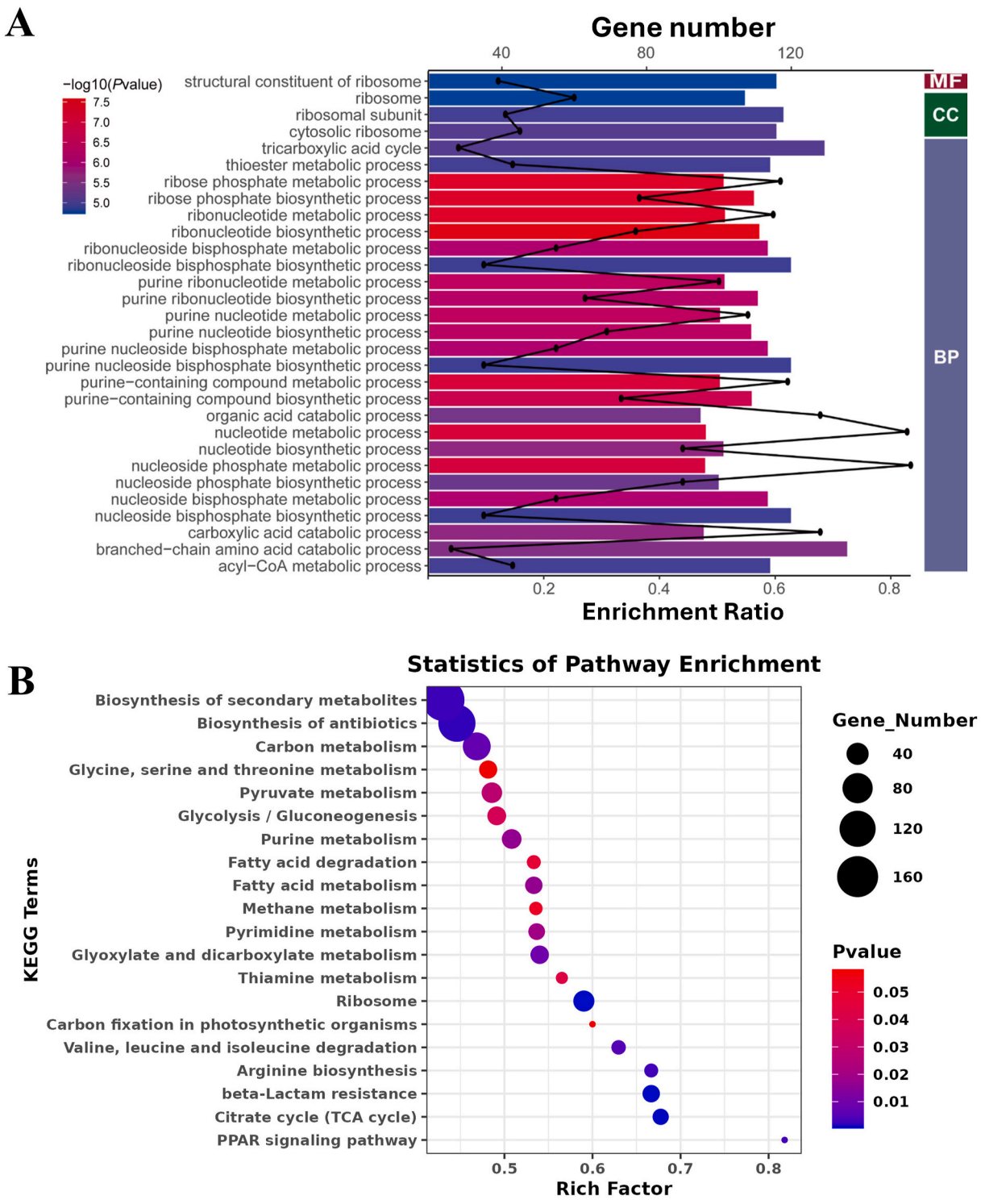

Fig. 7. GO classification of *B. cereus* DEGs (A) and scatter plots of enriched KEGG pathways for DEGs (B).

concentration used. This requires further study in the future.

4. Conclusions

This study showed that extracts from the five tested *T. sinensis* varieties had antibacterial activities against various *B. cereus* strains. Notably, the extracts from Sichuan Dazhu show particularly promising antibacterial activity against *B. cereus* strains, including those resistant to antibiotics. The primary constituents of Sichuan Dazhu extracts include flavonoids, amino acids and their derivatives, alkaloids, lipids, carbohydrates, polyphenols, and terpenoids. Moreover, Sichuan Dazhu extracts demonstrated antibiofilm activity against *B. cereus*. Transcriptome analysis revealed that the extracts impacted nucleic acid metabolism, protein metabolism, carbon metabolism, thiol metabolism, and metabolite synthesis, thereby exhibiting antibacterial effects against *B. cereus*. The extracts inhibited the attachment, microcolony development, maturation, and dispersion of *B. cereus* biofilm formation. Additionally, it exhibited antibacterial activity against *B. cereus* in skimmed milk. Therefore, *T. sinensis* extracts may be natural antibacterial agents for the control *B. cereus* in foods. In the future, it will be necessary to

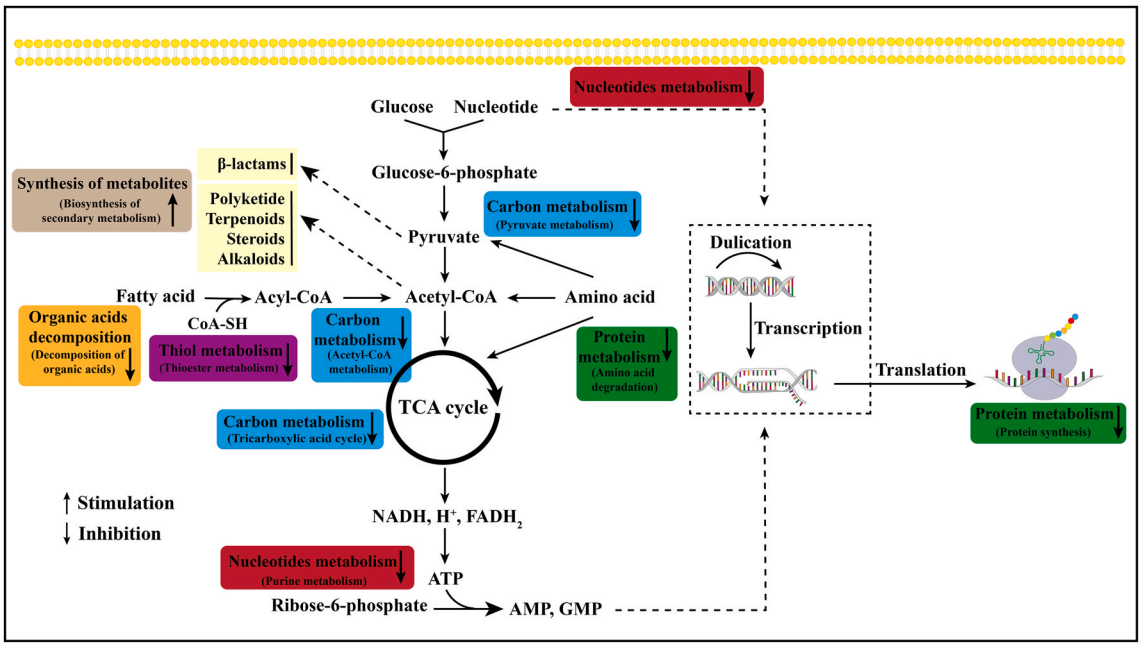

Fig. 8. Antibacterial mechanisms of *T. sinensis* extracts against *B. cereus*. The extracts affected the nucleic acid metabolism, protein metabolism, carbon metabolism, organic acids decomposition, thiol metabolism, and synthesis of metabolites in *B. cereus*.

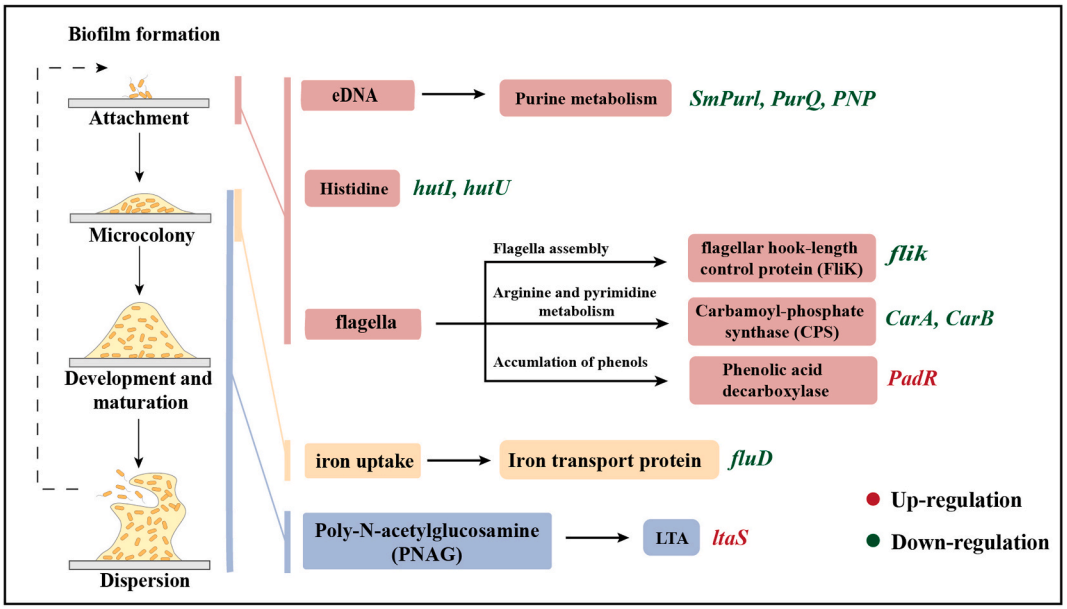

Fig. 9. Antibiofilm mechanisms of *T. sinensis* extracts against *B. cereus*. *T. sinensis* extracts disrupted various processes including eDNA synthesis, histidine synthesis, flagella synthesis and movement, iron metabolism, and lipoteichoic acid synthesis. These disruptions further impeded the attachment, microcolony formation, development and maturation, and dispersion of biofilm formation.

study the specific components responsible for the antibacterial and anti-biofilm properties of *T. sinensis* extracts.

CRediT authorship contribution statement

Yuru Wei: Software, Investigation, Visualization, Validation. **Lei Lei:** Investigation, Visualization, Validation. **Honglin Jiang:** Resources, Supervision, Project administration, Funding acquisition. **Qingquan Du:** Visualization, Validation. **Decheng Liu:** Conceptualization, Methodology. **Lu Chen:** Investigation, Resources. **Xiaoshan Shi:** Methodology, Resources. **Yanxiang Wang:** Investigation, Visualization. **Jingjing Li:** Project administration, Validation. **Yuanliang Hu:** Supervision, Project administration, Funding acquisition. **Xian Xia:** Methodology, Software, Investigation, Validation, Resources. **Junming Tu:** Conceptualization, Methodology, Resources, Supervision, Project administration, Funding acquisition.

Funding

This study was supported by the Hubei Provincial Central Committee Guides Local Special Projects (2023EGA041 and 2024BSB020), Hubei Province Key R&D Program Project (2022BCE010), National Natural Science Foundation of China (32000066), Natural Science Foundation of Hubei Province (2022CFB503, 2023AFB405), Innovation Team Project

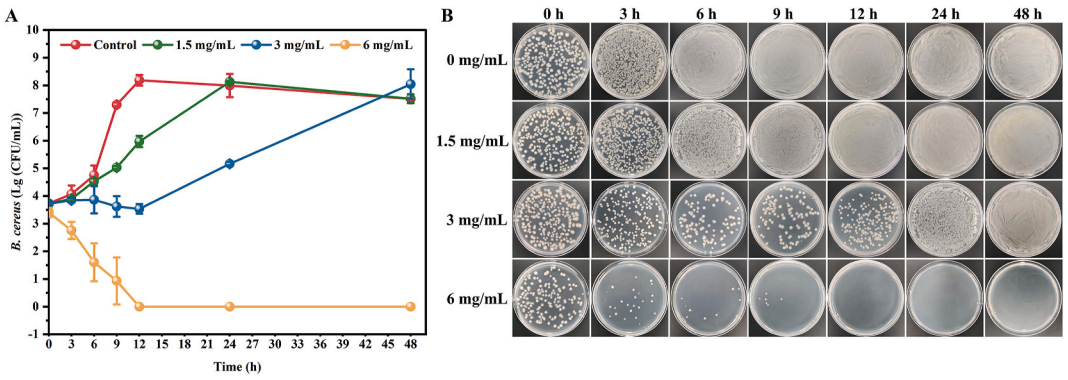

Fig. 10. Antibacterial activity of *T. sinensis* against extracts in skim milk. (A) The residue strains in skim milk treated with 0, 1.5, 3 and 6 mg/mL T. *sinensis* extracts. (B) Images of plates corresponding to different time points and concentrations of treatments as shown in (A).

of Hubei Education Department (T2022028), Huangshi City Health Research Project (WJ2024060), Open Foundation of the Hubei Key Laboratory of Edible Wild Plants Conservation and Utili-zation (EWPL202301 and EWPL202401).

Declaration of competing interest

The authors declare that they have no known competing financial interests or personal relationships that could have appeared to influence the work reported in this paper.

Appendix A. Supplementary data

Supplementary data to this article can be found online at https://doi.org/10.1016/j.crfs.2025.101045.

Data availability

The data that has been used is confidential.

References

Abouzeid, S., Beutling, U., Elekhnawy, E., Selmar, D., 2023. Antibacterial and antibiofilm effects of allelopathic compounds identified in *Medicago sativa* L. seedling exudate against *Escherichia coli*. Molecules 28, 2645. https://doi.org/10.3390/molecules28062645.

Adeyemo, R.O., Famuyide, I.M., Dzoyem, J.P., Lyndy Joy, M., 2022. Anti-biofilm, antibacterial, and anti-quorum sensing activities of selected South African plants traditionally used to treat diarrhoea. Evid-Based Compl. Alt. 2022, 1307801. https://doi.org/10.1155/2022/1307801.

Ahn, K.B., Baik, J.E., Yun, C.H., Han, S.H., 2018. Lipoteichoic acid inhibits *Staphylococcus aureus* biofilm formation. Front. Microbiol. 9, 327. https://doi.org/10.3389/fmicb.2018.00327.

Akinpelu, D.A., Aiyegoro, O.A., Akinpelu, O.F., Okoh, A.I., 2015. Stem bark extract and fraction of *Persea americana* (Mill.) exhibits bactericidal activities against strains of *Bacillus cereus* associated with food poisoning. Molecules 20, 416–429. https://doi.org/10.3390/molecules20010416.

Bai, J.-R., Zhong, K., Wu, Y.-P., Elena, G., Gao, H., 2019. Antibiofilm activity of shikimic acid against *Staphylococcus aureus*. Food Control 95, 327–333. https://doi.org/10.1016/j.foodcont.2018.08.020.

Balaban, M., Koc, C., Sar, T., Akbas, M.Y., 2021. Antibiofilm effects of pomegranate peel extracts against *B. cereus, B. subtilis*, and *E. faecalis*. J. Food Sci. Technol. 56, 4915–4924. https://doi.org/10.1111/ijfs.15221.

Bertuso, P.C., Marangon, C.A., Nitschke, M., 2022. Susceptibility of vegetative cells and endospores of *Bacillus cereus* to rhamnolipid biosurfactants and their potential application in dairy. Microorganisms 10. https://doi.org/10.3390/microorganisms10091860.

Bottone, E.J., 2010. *Bacillus cereus*, a volatile human pathogen. Clin. Microbiol. Rev. 23, 382–398. https://doi.org/10.1128/cmr.00073-09.

Buchmann, D., Schwabe, M., Weiss, R., Kuss, A.W., Schaufler, K., Schlüter, R., Rödiger, S., Guenther, S., Schultze, N., 2023. Natural phenolic compounds as biofilm inhibitors of multidrug-resistant *Escherichia coli* - the role of similar biological processes despite structural diversity. Front. Microbiol. 14, 1232039. https://doi.org/10.3389/fmicb.2023.1232039.

Caro-Astorga, J., Frenzel, E., Perkins, J.R., Álvarez-Mena, A., de Vicente, A., Ranea, J.A. G., Kuipers, O.P., Romero, D., 2020. Biofilm formation displays intrinsic offensive and defensive features of *Bacillus cereus*. npj Biofilms Microbiomes 6, 3. https://doi.org/10.1038/s41522-019-0112-7.

Chang, Y., Xia, S., Fei, P., Feng, H., Fan, F., Liu, Y., Qin, L., Ma, L., Song, Q., Liu, Y., 2023. *Houttuynia cordata* Thunb. crude extract inactivates *Cronobacter sakazakii*: antibacterial components, antibacterial mechanism, and application as a natural disinfectant. Food Control 145, 109467. https://doi.org/10.1016/j.foodcont.2022.109467.

Choi, W., Kim, S.S., 2020. Outbreaks, germination, and inactivation of *Bacillus cereus* in food products: a review. J. Food Prot. 83, 1480–1487. https://doi.org/10.4315/0362-028x.Jfp-19-429.

Diehl, F.F., Miettinen, T.P., Elbashir, R., Nabel, C.S., Darnell, A.M., Do, B.T., Manalis, S. R., Lewis, C.A., Vander Heiden, M.G., 2022. Nucleotide imbalance decouples cell growth from cell proliferation. Nat. Cell Biol. 24, 1252–1264. https://doi.org/10.1038/s41556-022-00965-1.

Ding, W., Zhou, Y., Qu, Q., Cui, W., God'spower, B.O., Liu, Y., Chen, X., Chen, M., Yang, Y., Li, Y., 2018. Azithromycin inhibits biofilm formation by *Staphylococcus xylosus* and affects histidine biosynthesis pathway. Front. Pharmacol. 9, 740. https://doi.org/10.3389/fphar.2018.00740.

Đukanović, S., Cvetković, S., Lončarević, B., Ljević, M., Nikolić, B., Simin, N., Bekvalac, K., Kekić, D., Mitić-Ćulafić, D., 2020. Antistaphylococcal and biofilm inhibitory activities of *Frangula alnus* bark ethyl-acetate extract. Ind. Crops Prod. 158, 113013. https://doi.org/10.1016/j.indcrop.2020.113013.

Fei, P., Xu, Y., Zhao, S., Gong, S., Guo, L., 2019. Olive oil polyphenol extract inhibits vegetative cells of *Bacillus cereus* isolated from raw milk. J. Dairy Sci. 102, 3894–3902. https://doi.org/10.3168/jds.2018-15184.

Fei, P., Sun, Z., Liu, X., Jiang, P., Feng, H., Chen, X., Ma, Y., Dong, G., Fan, C., Bai, M., Li, Y., Chang, Y., 2023. Antibacterial activity and mechanism of *Polygonatum sibiricum* extract against *Bacillus cereus* and its application in pasteurized milk. Foodborne Pathog. Dis. 21, 160–167. https://doi.org/10.1089/fpd.2023.0110.

Friedman, M., Henika, P.R., Levin, C.E., Mandrell, R.E., Kozukue, N., 2006. Antimicrobial activities of tea catechins and theaflavins and tea extracts against *Bacillus cereus*. J. Food Prot. 69, 354–361. https://doi.org/10.4315/0362-028X-69.2.354.

Fulde, M., Willenborg, J., Huber, C., Hitzmann, A., Willms, D., Seitz, M., Goethe, R., 2014. The arginine-ornithine antiporter ArcD contributes to biological fitness of *Streptococcus suis*. Front. Cell. Infect. Microbiol. 4, 107. https://doi.org/10.3389/fcimb.2014.00107.

Gan, R.Y., Kong, K.W., Li, H.B., Wu, K., Ge, Y.Y., Chan, C.L., Shi, X.M., Corke, H., 2018. Separation, identification, and bioactivities of the main gallotannins of red sword bean (*Canavalia gladiata*) coats. Front. Chem. 6, 39. https://doi.org/10.3389/fchem.2018.00039.

Gao, Z., Luan, Y., Yang, P., Wang, L., Zhang, H., Jing, S., Wang, L., Wang, T., Wang, D., 2020a. Targeting staphylocoagulase with isoquercitrin protects mice from Staphylococcus aureus–induced pneumonia. Appl. Microbiol. Biotechnol. 104, 3909–3919. https://doi.org/10.1007/s00253-020-10486-2.

Gao, Z., Zhong, W., Chen, K., Tang, P., Guo, J., 2020b. Chemical composition and anti-biofilm activity of essential oil from *Citrus medica* L. var. *sarcodactylis Swingle* against *Listeria monocytogenes*. Ind. Crops Prod. 144, 112036. https://doi.org/10.1016/j.indcrop.2019.112036.

Gélinas, M., Museau, L., Milot, A., Beauregard, P.B., 2021. The de novo purine biosynthesis pathway is the only commonly regulated cellular pathway during biofilm formation in TSB-based medium in *Staphylococcus aureus* and *Enterococcus faecalis*. Microbiol. Spectr. 9, e0080421. https://doi.org/10.1128/Spectrum.00804-21.

Gong, S., Jiao, C., Liu, B., Qu, W., Guo, L., Jiang, Y., 2023. Beetroot (*Beta vulgaris*) extract exerts an antibacterial effect by inducing apoptosis-like death in *Bacillus cereus*. J. Funct.Foods 105, 105571. https://doi.org/10.1016/j.jff.2023.105571.

Grau-Fuentes, E., Úbeda-Manzanaro, M., Martínez, A., Garzón, R., Rosell, C.M., Rodrigo, D., 2023. Evaluation of the antimicrobial activity of grape extract against *Bacillus cereus* in rice. LWT–Food Sci. Technol. 175, 114481. https://doi.org/10.1016/j.lwt.2023.114481.

Huang, Y.H., Huang, C.C., Chen, C.C., Yang, K.J., Huang, C.Y., 2015. Inhibition of *Staphylococcus aureus* PriA helicase by flavonol kaempferol. Protein J. 34, 169–172. https://doi.org/10.1007/s10930-015-9609-y.

Huang, Y., Flint, S.H., Palmer, J.S., 2020. *Bacillus cereus* spores and toxins – the potential role of biofilms. Food Microbiol. 90, 103493. https://doi.org/10.1016/j.fm.2020.103493.

Huang, Y., Flint, S.H., Loo, T.S., Palmer, J.S., 2022. Emetic toxin production of *Bacillus cereus* in a biofilm. LWT–Food Sci. Technol. 154, 112840. https://doi.org/10.1016/j.lwt.2021.112840.

Ivanov, M., Kannan, A., Stojkovic, D., Glamoclija, J., Golic Grdadolnik, S., Sanglard, D., Sokovic, M., 2020. Revealing the astragalin mode of anticandidal action. Excli j 19, 1436–1445. https://doi.org/10.17179/excli2020-2987.

Jovanovic, J., Ornelis, V.F.M., Madder, A., Rajkovic, A., 2021. *Bacillus cereus* food intoxication and toxicoinfection. Compr. Rev. Food Sci. Food Saf. 20, 3719–3761. https://doi.org/10.1111/1541-4337.12785.

Kaberdina, A.C., Ruiz-Larrabeiti, O., Lin-Chao, S., Kaberdin, V.R., 2019. Reprogramming of gene expression in *Escherichia coli* cultured on pyruvate versus glucose. Mol. Genet. Genom. 294, 1359–1371. https://doi.org/10.1007/s00438-019-01597-1.

Kang, J.-E., Liu, L., Wu, X., Sun, Y., Liu, Z.-L.J.A.M., 2018. Effect of thyme essential oil against *Bacillus cereus* planktonic growth and biofilm formation. Appl. Microbiol. Biotechnol. 102, 10209–10218. https://doi.org/10.1007/s00253-018-9401-y.

Koopman, J.A., Marshall, J.M., Bhatiya, A., Eguale, T., Kwiek, J.J., Gunn, J.S., 2015. Inhibition of *Salmonella enterica* biofilm formation using small-molecule adenosine mimetics. Antimicrob. Agents Chemother. 59, 76–84. https://doi.org/10.1128/aac.03407-14.

Kwong, W.K., Zheng, H., Moran, N.A., 2017. Convergent evolution of a modified, acetate-driven TCA cycle in bacteria. Nat. Microbiol. 2, 17067. https://doi.org/10.1038/nmicrobiol.2017.67.

Li, Y., Wang, M., Li, Y., Hong, B., Kang, D., Ma, Y., Wang, J., 2023. Two novel antimicrobial peptides against vegetative cells, spores and biofilm of *Bacillus cereus*. Food Control 149, 109688. https://doi.org/10.1016/j.foodcont.2023.109688.

Li, J., Liu, F.Y., He, B.L., Cui, R., Wu, H., 2025. Improving the bactericidal activity of carvacrol against *Bacillus cereus* by the formation of sodium casein-stabilized nanoemulsion and its application in milk preservation. Food Hydrocoll. 159, 110697. https://doi.org/10.1016/j.foodhyd.2024.110697.

Lim, A.C., Tang, S.G.H., Zin, N.M., Maisarah, A.M., Ariffin, I.A., Ker, P.J., Mahlia, T.M.I., 2022. Chemical composition, antioxidant, antibacterial, and antibiofilm activities of *Backhousia citriodora* essential oil. Molecules 27 (15), 4895. https://doi.org/10.3390/molecules27154895.

Lin, J., Zhou, D., Steitz, T.A., Polikanov, Y.S., Gagnon, M.G., 2018. Ribosome-targeting antibiotics: modes of action, mechanisms of resistance, and implications for drug design. Annu. Rev. Biochem. 87, 451–478. https://doi.org/10.1146/annurev-biochem-062917-011942.

Ling, N., Jiang, X., Forsythe, S., Zhang, D., Shen, Y., Ding, Y., Wang, J., Zhang, J., Wu, Q., Ye, Y., 2022. Food safety risks and contributing factors of *Cronobacter* spp. Engineering-PRC 12, 128–138. https://doi.org/10.1016/j.eng.2021.03.021.

Liu, X., Hu, W., An, Z., Bai, Z., Dai, X., Yang, Y., 2016. Exploration of cell lysis in a bioreactor using *Escherichia coli* expressing single-chain variable-domain antibody fragments. Ann. Microbiol. 66, 1207–1215. https://doi.org/10.1007/s13213-016-1202-x.

Liu, Z., Yuan, B., Zhao, L., Huang, L., Qin, Y., Zhang, J., Zhang, J., Hu, B., Yan, Q., 2022. Function of the *fliK* gene in *Pseudomonas plecoglossicida* pathogenicity and *Epinephelus coioides* immune response. Front. Mar. Sci. 9, 879333. https://doi.org/10.3389/fmars.2022.879333.

McCalley, S., Pirman, D., Clasquin, M., Johnson, K., Jin, S., Vockley, J., 2019. Metabolic analysis reveals evidence for branched chain amino acid catabolism crosstalk and the potential for improved treatment of organic acidurias. Mol. Genet. Metabol. 128, 57–61. https://doi.org/10.1016/j.ymgme.2019.05.008.

Memariani, H., Memariani, M., Ghasemian, A., 2019. An overview on anti-biofilm properties of quercetin against bacterial pathogens. World J. Microbiol. Biotechnol. 35, 143. https://doi.org/10.1007/s11274-019-2719-5.

Mlambo, L.K., Abbasiliasi, S., Tang, H.W., Ng, Z.J., Parumasivam, T., Hanafiah, K.M., Al-Shammary, A.A.K., Tan, J.S., 2022. Bioactive metabolites of *Lactiplantibacillus plantarum* K014 against Methicillin-Resistant *Staphylococcus aureus* ATCC43300 and in vitro evaluation of its antibacterial, antioxidant and anti-inflammatory activities. Curr. Microbiol. 79 (12), 359. https://doi.org/10.1007/s00284-022-03038-6.

Ning, Y., Ma, M., Zhang, Y., Zhang, D., Hou, L., Yang, K., Fu, Y., Wang, Z., Jia, Y., 2022. Antibacterial mechanism of sucrose laurate against *Bacillus cereus* by attacking multiple targets and its application in milk beverage. Food Rev. Int. 154, 111018. https://doi.org/10.1016/j.foodres.2022.111018.

Park, S.C., Kwak, Y.M., Song, W.S., Hong, M., Yoon, S.-i, 2017. Structural basis of effector and operator recognition by the phenolic acid-responsive transcriptional regulator PadR. Nucleic Acids Res. 45, 13080–13093. https://doi.org/10.1093/nar/gkx1055.

Pawluk, A.M., Kim, D., Jin, Y.H., Jeong, K.C., Mah, J.-H., 2022. Biofilm-associated heat resistance of *Bacillus cereus* spores in vitro and in a food model, *Cheonggukjang jjigae*. Int. Food Res. J. 363, 109505. https://doi.org/10.1016/j.ijfoodmicro.2021.109505.

Peng, W., Liu, Y., Hu, M., Zhang, M., Yang, J., Liang, F., Huang, Q., Wu, C., 2018. *Toona sinensis*: a comprehensive review on its traditional usages, phytochemisty, pharmacology and toxicology. Rev. Bras. Farmacogn. 29, 111–124. https://doi.org/10.1016/j.bjp.2018.07.009.

Ren, X., An, P., Zhai, X., Wang, S., Kong, Q., 2019. The antibacterial mechanism of pterostilbene derived from xinjiang wine grape: a novel apoptosis inducer in *Staphyloccocus aureus* and *Escherichia coli*. LWT–Food Sci. Technol. 101, 100–106. https://doi.org/10.1016/j.lwt.2018.11.038.

Shamsudin, N.F., Ahmed, Q.U., Mahmood, S., Ali Shah, S.A., Khatib, A., Mukhtar, S., Alsharif, M.A., Parveen, H., Zakaria, Z.A., 2022. Antibacterial effects of flavonoids and their structure-activity relationship study: a comparative interpretation. Molecules 27, 1149. https://doi.org/10.3390/molecules27041149.

Son, J., Lee, S.Y., 2020. Therapeutic potential of ursonic acid: comparison with ursolic acid. Biomolecules 10, 1505. https://doi.org/10.3390/biom10111505.

Su, S., Wang, L., Ni, J., Geng, Y., Xu, X., 2020. Diversity of red, green and black cultivars of Chinese Toon [*Toona sinensis* (A. Juss.) Roem]: anthocyanins, flavonols and antioxidant activity. J. Food Meas. Char. 14, 3206–3215. https://doi.org/10.1007/s11694-020-00560-8.

Sun, X.-h., Hao, L.-r., Xie, Q.-c., Lan, W.-q., Zhao, Y., Pan, Y.-j., Wu, V.C.H., 2020. Antimicrobial effects and membrane damage mechanism of blueberry (*Vaccinium corymbosum* L.) extract against *Vibrio parahaemolyticus*. Food Control 111, 107020. https://doi.org/10.1016/j.foodcont.2019.107020.

Tian, Q., Wei, S., Su, H., Zheng, S., Xu, S., Liu, M., Bo, R., Li, J., 2022. Bactericidal activity of gallic acid against multi-drug resistance *Escherichia coli*. Microb. Pathog. 173, 105824. https://doi.org/10.1016/j.micpath.2022.105824.

Tritripmongkol, P., Sangkanu, S., Boripun, R., Jeenkeawpieam, J., Chuprom, J., Nissapatorn, V., Pereira, M.L., Paul, A.K., Mitsuwan, W., 2022. Robusta coffee extracts inhibit quorum sensing activity in *Chromobacterium violaceum* and reduce biofilms against *Bacillus cereus* and *Staphylococcus aureus*. Vet. World 15, 2391–2398. https://doi.org/10.14202/vetworld.2022.2391-2398.

Truong, L., Hevener, K.E., Rice, A.J., Patel, K., Johnson, M.E., Lee, H., 2013. High-level expression, purification, and characterization of *Staphylococcus aureus* dihydroorotase (PyrC) as a cleavable His-SUMO fusion. Protein Expr. Purif. 88 (1), 98–106. https://doi.org/10.1016/j.pep.2012.11.018.

Tuipulotu, D.E., Mathur, A., Ngo, C., Man, S.M., 2021. *Bacillus cereus*: epidemiology, virulence factors, and host–pathogen interactions. Trends Microbiol. 29, 458–471. https://doi.org/10.1016/j.tim.2020.09.003.

Wang, K.-J., Yang, C.-R., Zhang, Y.-J., 2007. Phenolic antioxidants from Chinese toon (fresh young leaves and shoots of *Toona sinensis*). Food Chem. 101, 365–371. https://doi.org/10.1016/j.foodchem.2006.01.044.

Wang, N., Sadiq, F.A., Li, S., He, G., Yuan, L., 2020. Tandem mass tag-based quantitative proteomics reveals the regulators in biofilm formation and biofilm control of *Bacillus licheniformis*. Food Control 110, 107029. https://doi.org/10.1016/j.foodcont.2019.107029.

Wang, T., Zhang, P., Lv, H., Deng, X., Wang, J., 2020. A natural dietary flavone myricetin as an α-hemolysin inhibitor for controlling *Staphylococcus aureus* infection. Front. Cell. Infect. Microbiol. 10, 330. https://doi.org/10.3389/fcimb.2020.00330.

Wang, X., Tian, L., Fu, J., Liao, S., Yang, S., Jia, X., Gong, G., 2022. Evaluation of the membrane damage mechanism of thymol against *Bacillus cereus* and its application in the preservation of skim milk. Food Control 131, 108435. https://doi.org/10.1016/j.foodcont.2021.108435.

Wang, Y., Yang, H., Geerts, C., Furtos, A., Waters, P., Cyr, D., Wang, S., Mitchell, G.A., 2023. The multiple facets of acetyl-CoA metabolism: energetics, biosynthesis, regulation, acylation and inborn errors. Mol. Genet. Metabol. 138, 106966. https://doi.org/10.1016/j.ymgme.2022.106966.

Wilson, D.J., Middleton, J.R., Adkins, P.R.F., Goodell, G.M., 2019. Test agreement among biochemical methods, matrix-assisted laser desorption ionization–time of flight mass spectrometry, and 16S rRNA sequencing for identification of microorganisms isolated from bovine milk. J. Clin. Microbiol. 57. https://doi.org/10.1128/jcm.01381-18.

Xu, N., Du, L.H., Chen, Y.C., Zhang, J.H., Zhu, Q.F., Chen, R., Peng, G.P., Wang, Q.M., Yu, H.Z., Rao, L.Q., 2023. *Lonicera japonica* Thunb. as a promising antibacterial agent for *Bacillus cereus* ATCC14579 based on network pharmacology, metabolomics, and in vitro experiments. RSC Adv. 13, 15379–15390. https://doi.org/10.1039/d3ra00802a.

Yang, Z., Li, L., Chen, C.H., Zhang, Y.Y., Yang, Y., Zhang, P., Bao, G.H., 2022. Chemical composition and antibacterial activity of 12 medicinal plant ethyl acetate extracts using LC-MS feature-based molecular networking. Phytochem. Anal. 33, 473–489. https://doi.org/10.1002/pca.3103.

Yang, S., Wang, Y., Ren, F., Li, Z., Dong, Q., 2023. Applying enzyme treatments in *Bacillus cereus* biofilm removal. LWT–Food Sci. Technol. 180, 114667. https://doi.org/10.1016/j.lwt.2023.114667.

Zaunmüller, T., Eichert, M., Richter, H., Unden, G., 2006. Variations in the energy metabolism of biotechnologically relevant heterofermentative lactic acid bacteria during growth on sugars and organic acids. Appl. Microbiol. Biotechnol. 72, 421–429. https://doi.org/10.1007/s00253-006-0514-3.

Zhang, R., Abdel-Motaal, H., Zou, Q., Guo, S., Zheng, X., Wang, Y., Zhang, Z., Meng, L., Xu, T., Jiang, J., 2020. A novel MFS-MDR transporter, MdrP, employs D223 as a key determinant in the Na^+ translocation coupled to norfloxacin efflux. Front. Microbiol. 11, 955. https://doi.org/10.3389/fmicb.2020.00955.

Zhang, Y., Pan, X., Wang, L., Chen, L., 2021. Iron metabolism in *Pseudomonas aeruginosa* biofilm and the involved iron-targeted anti-biofilm strategies. J. Drug Target. 29, 249–258. https://doi.org/10.1080/1061186x.2020.1824235.

Zhang, Z., Guo, Y., Guo, Y., Zhang, L., Niu, S., Tian, C., Han, L., Zhang, D., Liu, M., 2022. Molecular basis for luteolin as a natural TatD DNase inhibitor in *Trueperella pyogenes*. Int. J. Mol. Sci. 23, 8374. https://doi.org/10.3390/ijms23158374.

Zhao, Q., Zhong, X.L., Zhu, S.H., Wang, K., Tan, G.F., Meng, P.H., Zhang, J., 2022. Research advances in *Toona sinensis*, a traditional Chinese medicinal plant and popular vegetable in China. Agronomy 14, 572. https://doi.org/10.3390/d14070572.

Zhao, Q., Zhong, X.L., Cai, X., Zhu, S.H., Meng, P.-H., Zhang, J., Tan, G.F., 2023. Comparative physiological analysis of lignification, anthocyanin metabolism and correlated gene expression in red *Toona sinensis* buds during cold storage. Agronomy 13, 119. https://doi.org/10.3390/agronomy13010119.

Zheng, Y., Ye, J., Xie, Y.G., Li, H.L., Jin, H.Z., 2017. Chemical constituents of *Dysosma versipellis*. Chem. Nat. Compd. 53, 151–153. https://doi.org/10.1007/s10600-017-1933-3.

Zhou, H., Chen, L., Ouyang, K., Zhang, Q., Wang, W., 2023. Antibacterial activity and mechanism of flavonoids from *Chimonanthus salicifolius* S. Y. Hu. and its transcriptome analysis against *Staphylococcus aureus*. Front. Microbiol. 13, 1103476. https://doi.org/10.3389/fmicb.2022.1103476.

Zhu, F., Peña, M., Bennett, G.N., 2021. Metabolic engineering of *Escherichia coli* for quinolinic acid production by assembling L-aspartate oxidase and quinolinate synthase as an enzyme complex. Metab. Eng. 67, 164–172. https://doi.org/10.1016/j.ymben.2021.06.007.

Zhuo, T., Rou, W., Song, X., Guo, J., Fan, X., Kamau, G.G., Zou, H., 2015. Molecular study on the carAB operon reveals that carB gene is required for swimming and biofilm formation in *Xanthomonas citri* subsp. citri. BMC Microbiol. 15, 225. https://doi.org/10.1186/s12866-015-0555-9.